

Unified description of nuclear matter properties within the CBF effective interaction approach

Omar Benhar¹ and Alessandro Lovato²

¹INFN and Dipartimento di Fisica, Sapienza University, I-00185 Rome, Italy

²Physics Division, Argonne National Laboratory, Argonne, IL 60439

E-mail: ¹omar.benhar@roma1.infn.it

E-mail: ²lovato@anl.gov

Abstract. We discuss the derivation of an effective interaction, obtained from a realistic nuclear Hamiltonian using the formalism of Correlated Basis Functions (CBF) and the cluster expansion technique. Unlike the bare nucleon-nucleon potential, the CBF effective interaction is well behaved, and suitable for carrying out perturbative calculations in the basis of eigenstates of the non interacting system. The results of studies of a variety of properties of nuclear matter, at both zero and nonzero temperatures, are reported and analyzed.

1. Introduction

This paper will focus on the tiny—although arguably most important—region of the QCD phase diagram corresponding to vanishing or very low temperatures and densities comparable to the central density of atomic nuclei, $\rho_0 = 0.16 \text{ fm}^{-3}$. Under these conditions, the ground state of strongly-interacting matter is known to consist of protons and neutrons, the interactions of which can be described by a non relativistic Hamiltonian.

In the case of isospin-symmetric nuclear matter (SNM)—that is, a translation invariant system with equal numbers of protons and neutrons interacting through nuclear forces only—the binding energy per particle can be determined from the extrapolation of the nuclear mass formula, yielding the result $E_0 \approx -16 \text{ MeV}$. Additional information can be extracted from measurements of nuclear properties and nuclear reactions, giving access to quantities such as the compression modulus, $K \approx 260 \pm 30 \text{ MeV}$, and the symmetry energy, $E_{\text{sym}} \approx 31.6 \pm 2.66$.

Effective interactions specifically designed to reproduce the available empirical information on SNM (see, e.g., Refs. [1, 2]), while being remarkably successful in a number of instances, are limited by the lack of a connection with nuclear dynamics at microscopic level. As a consequence, they are inherently unable to provide a quantitative account of nucleon-nucleon scattering processes—both in free space and in the nuclear medium—whose understanding is needed for the description of non-equilibrium properties [3, 4].

Early attempts to derive an effective interaction from a phenomenological nucleon-nucleon potential are described in Refs.[5, 6]. More recently, the authors of Refs. [7, 8] have improved on the approach of Ref. [5], and developed a procedure to determine the effective interaction using the Correlated Basis Function (CBF) formalism and the cluster expansion technique.

The results of extensive studies of the Fermi hard-sphere system strongly suggest that the CBF effective interaction approach provides accurate estimates of a variety of fundamental



quantities of interacting many-body systems other than the ground-state energy, such as the self-energy determining the two-point Green's function [9, 10].

The applications to nuclear matter, discussed in this paper, include calculations of a number of properties of great astrophysical interest, such as the equation of state, the quasiparticle spectrum and the chemical potentials of uniform matter at fixed baryon density and large neutron excess, at both zero and nonzero temperature.

The main features of the nuclear Hamiltonian and the derivation of the CBF effective interaction are described in Section 2, while Section 3 is devoted to the discussion of numerical results, including the ground-state energy at arbitrary proton fraction, the symmetry energy, the pressure and the single-nucleon spectrum. Finally, in Section 4 we summarize our findings, and outline the prospects for future applications of the approach.

2. Theoretical framework

In this section, we will outline the phenomenological model of nuclear dynamics employed to obtain the numerical results, and describe the procedure leading to the determination of the effective interaction.

2.1. The nuclear Hamiltonian

Within non relativistic many-body theory (NMBT) atomic nuclei, as well as infinite nuclear matter, are described in terms of point-like nucleons of mass m , whose dynamics are dictated by the Hamiltonian

$$H = \sum_i -\frac{\nabla_i^2}{2m} + \sum_{i<j} v_{ij} + \sum_{i<j<k} V_{ijk}. \quad (1)$$

The nucleon-nucleon (NN) potential v_{ij} is obtained from an accurate fit of the measured properties of the two-nucleon system—in both bound and scattering states—and reduces to the Yukawa one-pion-exchange potential at large distances. Coordinate-space NN potentials are usually written in the form

$$v_{ij} = \sum_p v^p(r_{ij}) O_{ij}^p, \quad (2)$$

where $r_{ij} = |\mathbf{r}_i - \mathbf{r}_j|$ is the distance between the interacting particles, and the sum includes up to eighteen terms. The most prominent contributions are those associated with the operators

$$O_{ij}^{p \leq 6} = [1, (\boldsymbol{\sigma}_i \cdot \boldsymbol{\sigma}_j), S_{ij}] \otimes [1, (\boldsymbol{\tau}_i \cdot \boldsymbol{\tau}_j)], \quad (3)$$

where $\boldsymbol{\sigma}_i$ and $\boldsymbol{\tau}_i$ are Pauli matrices acting in spin and isospin space, respectively, while the operator

$$S_{ij} = \frac{3}{r_{ij}^2} (\boldsymbol{\sigma}_i \cdot \mathbf{r}_{ij})(\boldsymbol{\sigma}_j \cdot \mathbf{r}_{ij}) - (\boldsymbol{\sigma}_i \cdot \boldsymbol{\sigma}_j), \quad (4)$$

accounts for the occurrence of non-spherically-symmetric interactions. The potentials obtained including the six operators of Eqs. (3)-(4) explain deuteron properties and the S -wave scattering phase shifts. In order to describe the P -wave, one has to include two additional components involving the momentum dependent operators

$$O_{ij}^{p=7,8} = (\boldsymbol{\ell} \cdot \mathbf{S}), (\boldsymbol{\ell} \cdot \mathbf{S})(\boldsymbol{\tau}_1 \cdot \boldsymbol{\tau}_2), \quad (5)$$

where $\boldsymbol{\ell}$ denotes the angular momentum of the relative motion of the interacting particles.

The operators corresponding to $p = 7, \dots, 14$ are associated with the non-static components of the NN interaction, while those corresponding to $p = 15, \dots, 18$ account for small violations of charge symmetry. All these terms are included in the state-of-the-art Argonne v_{18} (AV18) potential [11], providing a fit of the scattering data collected in the Nijmegen database, the low-energy nucleon-nucleon scattering parameters and deuteron properties with a reduced chi-square $\chi^2 \simeq 1$.

The results reported in this paper have been obtained using the so-called Argonne v'_6 (AV6P) interaction, which is not simply a truncated version of the full AV18 potential—obtained neglecting the contributions with $p > 6$ in Eq. (2)—but rather its reprojection on the basis of the six spin-isospin operators of Eqs. (3)-(4) [12].

The inclusion of the additional three-nucleon (NNN) term, V_{ijk} , is needed to explain the binding energies of the three-nucleon systems and the saturation properties of SNM. The derivation of V_{ijk} was first discussed in the pioneering work of Fujita and Miyazawa [13]. They argued that its main component originates from two-pion-exchange processes in which a NN interaction leads to the excitation of one of the participating nucleons to a Δ resonance, which then decays in the aftermath of the interaction with a third nucleon. Commonly used phenomenological models of the NNN force, like the Urbana IX (UIX) potential [14], are written in the form

$$V_{ijk} = V_{ijk}^{2\pi} + V_{ijk}^N, \quad (6)$$

where $V_{ijk}^{2\pi}$ is the attractive Fujita-Miyazawa term, while V_{ijk}^N is a purely phenomenological repulsive term. The parameters entering the definition of the above potential are adjusted in such a way as to reproduce the ground state energy of the three-nucleon systems and the equilibrium density of SNM, when used in conjunction with the AV18 NN interaction.

Note that within the framework of NMBT the determination of the nuclear Hamiltonian implies very little theoretical bias, because the two- and three-nucleon systems are solved exactly, and the equilibrium properties of SNM can be computed with great accuracy.

It has to be emphasized that local NN potentials derived within the alternate framework of chiral perturbation theory are also written in the form of Eq. (2) [15, 16]. Since local versions of the chiral NNN potentials [17] have the same spin-isospin structure of the UIX force, the scheme described in this paper can be readily applied using chiral nuclear Hamiltonians.

2.2. Derivation of the CBF effective interaction

The formalism of Correlated Basis Functions (CBF) is based on the variational approach to the many-body problem with strong forces, first proposed by R. Jastrow back in the 1950s [18]. Within this scheme, the trial ground state of the nuclear hamiltonian is written in the form

$$|\Psi_0\rangle \equiv \frac{\mathcal{F}|\Phi_0\rangle}{\langle\Phi_0|\mathcal{F}^\dagger\mathcal{F}|\Phi_0\rangle^{1/2}}, \quad (7)$$

where $|\Phi_0\rangle$ is a Slater determinant built from single particle states $|\phi_\alpha\rangle$, with $\{\alpha\}$ being the set of quantum numbers of the states belonging to the Fermi sea. In the case of uniform matter at density $\rho = \nu k_F^3/(6\pi^2)$ —where k_F and ν denote the Fermi momentum and the degeneracy of the momentum eigenstates, respectively— $|\phi_\alpha\rangle$ consists of a plane wave, with momentum \mathbf{k} such that $|\mathbf{k}| \leq k_F$, and the Pauli spinors associated with the spin and isospin degrees of freedom.

The many-body operator \mathcal{F} , describing the effects of correlations among the nucleons, is written as a product of two-body operators, whose structure mirrors that of the AV6P potential, as

$$\mathcal{F} \equiv \mathcal{S} \prod_{i<j} F_{ij}, \quad (8)$$

with

$$F_{ij} = \sum_{p=1}^6 f^p(r_{ij}) O_{ij}^p . \quad (9)$$

Note that the symmetrization operator \mathcal{S} is needed to fulfill the requirement of antisymmetrization of $|\Psi_0\rangle$ under particle exchange, since, in general, $[O_{ij}^p, O_{jk}^q] \neq 0$.

The radial dependence of the correlation functions $f^p(r_{ij})$, determined from functional minimization of the expectation value of the Hamiltonian in the correlated ground state,

$$E_V = \langle \Psi_0 | H | \Psi_0 \rangle . \quad (10)$$

is largely shaped by the strongly repulsive core of the NN interaction, resulting in a drastic suppression of the probability to find two nucleons at relative distance $r_{ij} \lesssim 1$ fm. Longer range correlations, mainly due to the non-central components of the NN potential, are also important.

The calculation of the variational energy of Eq. (10) involves severe difficulties. It can be efficiently carried out expanding the right-hand side in a series, whose terms describe the contributions of clusters involving an increasing number of correlated particles [19]. The terms of the cluster expansion can be represented by diagrams, and classified according to their topological structures. Selected classes of diagrams can then be summed to all orders solving a set of coupled non-linear integral equations, referred to as Fermi Hyper-Netted Chain/Single-Operator Chain (FHNC/SOC) equations [20, 21], to obtain an accurate estimate of the ground state energy.

Under the assumption that the correlation structure of the ground and excited states of the system be the same, the operator \mathcal{F} obtained from the variational calculation of E_V can be used to generate correlated excited states from Eq. (7) by replacing $|\Phi_0\rangle \rightarrow |\Phi_n\rangle$, with $|\Phi_n\rangle$ being any eigenstate of the non interacting Fermi gas. The resulting correlated states span a complete, although non orthogonal, set, that can be used to carry out perturbative calculations within the scheme developed in Ref. [22]. This approach, known as CBF perturbation theory, has been successfully applied to study a variety of nuclear matter properties, including the response functions [23, 24] and the two-point Green's function [25, 26].

In CBF perturbation theory, one has to evaluate matrix elements of the *bare* nuclear Hamiltonian, the effects of correlations being taken into account by the transformation of the basis states describing the non interacting system. However, the same result can in principle be obtained transforming the Hamiltonian, and using the Fermi gas basis. This procedure leads to the appearance of an *effective* Hamiltonian suitable for use in standard perturbation theory, thus avoiding the non trivial difficulties arising from the use of a non-orthogonal basis [27].

The CBF effective interaction is defined through the matrix element of the bare Hamiltonian in the correlated ground state, according to

$$\langle \Psi_0 | H | \Psi_0 \rangle = T_F + \langle \Phi_0 | \sum_{i<j} v_{ij}^{\text{eff}} | \Phi_0 \rangle , \quad (11)$$

where T_F denotes the energy of the non interacting Fermi gas, and the effective potential is written in terms of the same spin-isospin operators appearing in Eq. (2)

$$v_{ij}^{\text{eff}} = \sum_p v^{\text{eff},p}(r_{ij}) O_{ij}^p . \quad (12)$$

From the above equation, it is apparent that v_{ij}^{eff} embodies the effect of correlations. As a consequence, it is well behaved at short distances, and can in principle be used to carry out perturbative calculations of any properties of nuclear matter.

The authors of Ref. [7] first proposed to obtain the effective interaction performing a cluster expansion of the left-hand side of Eq. (11) and keeping the two-body cluster contribution only. While leading to a very simple and transparent expression for v_{ij}^{eff} , however, this scheme was seriously limited by its inability to take into account the NNN potential V_{ijk} . In Ref. [8] the effects of interactions involving more than two nucleons have been included through a density-dependent modification of the NN potential at intermediate range [28].

A significant improvement has been achieved by the authors of Refs. [29, 30], who explicitly took into account three-nucleon cluster contributions to the ground-state energy. This procedure allows to describe the effects of three-nucleon interactions at fully microscopic level using the UIX potential.

Note that the correlation functions $f^p(r_{ij})$ entering the definition of v_{ij}^{eff} are *not* the same as those obtained from the minimization of the variational energy of Eq. (10). They are adjusted so that the ground state energy computed at first order in v_{ij}^{eff} —that is, in the Hartree-Fock approximation—reproduces the value of E_V resulting from the full FHNC/SOC calculation. In Refs. [29] and [30], this procedure was applied, *separately*, to SNM and pure neutron matter (PNM). The effective interaction employed to obtain the results discussed in this paper, on the other hand, simultaneously describes the density dependence of the energy per nucleon of *both* SNM and PNM. This feature is essential for astrophysical applications, because it allows to evaluate the properties of nuclear matter at fixed baryon density and large neutron excess, which is believed to make up a large region of the neutron star interior.

3. Nuclear Matter Properties

3.1. Ground state energy of cold nuclear matter

The procedure developed by the authors of Ref. [31, 32], taking into account the contributions of three-nucleon clusters, allows to use a realistic nuclear Hamiltonian, comprising two- and three-nucleon potentials. The results reported in this paper have been obtained combining the AV6P [33] and UIX [34] potentials.

The resulting effective interaction—derived using as baseline the FHNC variational estimates of the ground state energy of PNM and SNM—can be used to evaluate the energy per nucleon of neutron rich and spin polarized matter at fixed baryon density

$$\rho = \sum_{\lambda} \rho_{\lambda} = \rho \sum_{\lambda} x_{\lambda}, \quad (13)$$

where the index $\lambda = 1, 2, 3, 4$ labels spin-up protons, spin-down protons, spin-up neutrons and spin-down neutrons, respectively, the corresponding densities being $\rho_{\lambda} = x_{\lambda}\rho$. In SNM $x_1 = x_2 = x_3 = x_4 = 1/4$, while in PNM $x_1 = x_2 = 0$ and $x_3 = x_4 = 1/2$.

At first order in the CBF effective interaction, the energy per baryon can be written in the form

$$\frac{E}{A} = \frac{3}{5} \sum_{\lambda} x_{\lambda} \frac{k_{F\lambda}^2}{2m} + \frac{\rho}{2} \sum_{\lambda\mu} x_{\lambda} x_{\mu} \int d^3r \left[v_{\lambda\mu}^{\text{eff,d}}(r) - v_{\lambda\mu}^{\text{eff,e}}(r) \ell(k_{F\lambda} r) \ell(k_{F\mu} r) \right] \quad (14)$$

where $v_{\lambda\mu}^{\text{eff,d}}(r)$ and $v_{\lambda\mu}^{\text{eff,e}}(r)$ denote the direct and exchange matrix elements of the effective interaction in spin-isospin space, $k_{F\lambda} = (6\pi^2\rho_{\lambda})^{1/3}$ is the Fermi momentum of the nucleons of type λ and

$$\rho_{\lambda} \ell(k_{F\lambda} r) \equiv \frac{1}{V} \sum_{\mathbf{k}} e^{i\mathbf{k}\cdot\mathbf{r}} n_{\lambda}(\mathbf{k}), \quad (15)$$

with $n_{\lambda}(\mathbf{k}) = \theta(k_{F\lambda} - |\mathbf{k}|)$ and V being is the zero-temperature Fermi distribution and the normalization volume, respectively.

The solid lines of Figures 1 and 2 illustrate the density dependence of the energy per nucleon of PNM and SNM, respectively, obtained from Eq. (14) using the CBF effective interaction. The shaded regions show the FHNC results obtained using the bare Hamiltonian, with the associated theoretical uncertainty arising from the treatment of the kinetic energy [35]. For comparison, the results of a calculation carried out using the Auxiliary Field Diffusion Monte Carlo (AFDMC) [36] technique are also displayed. It clearly appears that the FHNC variational estimates provide a very accurate upper bound to the ground state energy. Note, however, that while the empirical equilibrium density of SNM is well reproduced, the corresponding energy is underestimated by ~ 5 MeV.

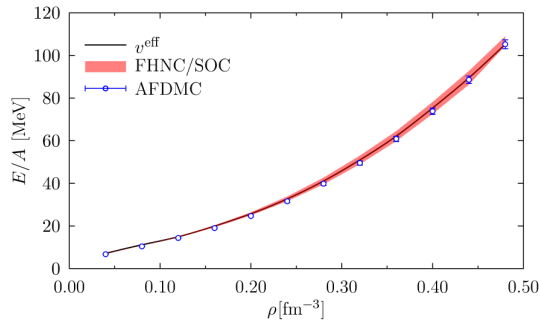


Figure 1. Density dependence of the energy per nucleon of PNM. The solid lines display results obtained using Eqs. (14)-(15) and the CBF effective interaction. The variational FHNC results are represented by the shaded regions, accounting for the uncertainty arising from the treatment of the kinetic energy, while the open circles correspond to the results obtained using the AFDMC technique.

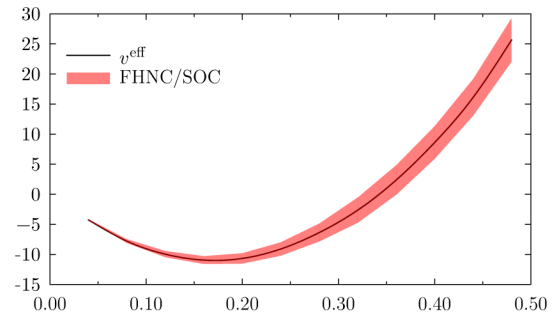


Figure 2. Density dependence of the energy per nucleon of SNM. The solid lines display results obtained using Eqs. (14)-(15) and the CBF effective interaction. The variational FHNC results are represented by the shaded regions, accounting for the uncertainty arising from the treatment of the kinetic energy.

The main advantage of the effective interaction approach is the possibility of carrying out calculations of a variety of nuclear matter properties of astrophysical interest using perturbation theory and the orthogonal basis of eigenstates of the non interacting system. Of great importance, in this context, is the ground state energy of matter at fixed baryon density and arbitrary proton fraction, $x_p = x_1 + x_2$, shown in Fig. 3 for $0 \leq x_p \leq 0.5$.

3.2. Symmetry energy

Consider again unpolarized matter with proton and neutron densities $\rho_p = x_p \rho$ and $\rho_n = (1 - x_p) \rho$, respectively. The ground-state energy per nucleon can be expanded in series of powers of the quantity $\delta = (\rho_n - \rho_p) / \rho$, providing a measure of neutron excess. The resulting expression reads (see, e.g., Ref. [37])

$$\frac{1}{A} E_0(\rho, \delta) = \frac{1}{A} E_0(\rho, 0) + E_{\text{sym}}(\rho) \delta^2 + O(\delta^4), \quad (16)$$

where the symmetry energy

$$E_{\text{sym}}(\rho) = \left\{ \frac{\partial^2 [E_0(\rho, \delta) / A]}{\partial \delta^2} \right\}_{\delta=0} \quad (17)$$

$$\approx \frac{1}{A} E_0(\rho, 1) - \frac{1}{A} E_0(\rho, 0)$$

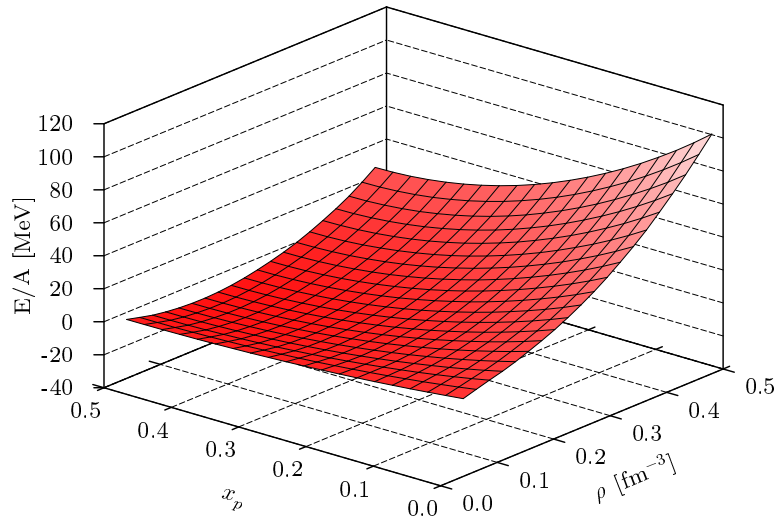


Figure 3. Energy per nucleon of uniform nuclear matter, computed as a function of baryon density, ρ , and proton fraction, $x_p = x_1 + x_2$, using Eqs. (14)-(15) and the CBF effective interaction.

can be interpreted as the energy required to convert SNM into PNM. The density dependence of $E_{\text{sym}}(\rho)$, that can be obtained expanding around the equilibrium density, is conveniently characterized by the quantity

$$L = 3\rho_0 \left(\frac{dE_{\text{sym}}}{d\rho} \right)_{\rho=\rho_0}. \quad (18)$$

Empirical information on $E_{\text{sym}}(\rho_0)$ and L have been extracted from data collected by laboratory experiments and astrophysical observations [38]. The values resulting from our calculations, $E_{\text{sym}}(\rho_0) = 30.9$ MeV and $L = 67.9$ MeV, turn out to be compatible with those obtained from a survey of 28 analyses, carried out by the authors of Ref. [38], yielding $E_{\text{sym}}(\rho_0) = 31.6 \pm 2.66$ and $L = 58.9 \pm 16$ MeV.

The density dependence of the symmetry energy has been recently discussed in Ref. [39], whose authors combined the results of isospin-dependent flow measurements carried out by the ASY-EOS Collaboration at GSI with those obtained from analyses of low-energy heavy-ion collisions [40] and nuclear structure studies [41, 42, 43].

Figure 4 shows a comparison between $E_{\text{sym}}(\rho)$ resulting from our calculations and the empirical information reported in Refs. [38, 39, 40, 41, 42, 43]. It appears that theoretical results are compatible with experiments at most densities.

3.3. Pressure

The pressure of nuclear matter, which plays a critical role in determining the properties of the equilibrium configurations of neutron stars, is simply related to the the ground-state energy through

$$P = - \left(\frac{\partial E_0}{\partial V} \right)_A = \rho^2 \frac{\partial(E_0/A)}{\partial \rho}, \quad (19)$$

where the derivative is taken keeping the number of nucleons constant.

The dashed line of Fig. 5 illustrates the density dependence of the pressure of SNM obtained from our approach. For comparison, the shaded area also shows the region consistent with the experimental flow data discussed in Ref. [44], providing a constraint on $P(\rho)$ at $\rho \geq 2\rho_0$. It appears while being within the allowed boundary at $2\rho_0 \leq \rho \leq 3\rho_0$, the calculated pressure exhibits a slope suggesting that a discrepancy may occur at higher density. However, in this

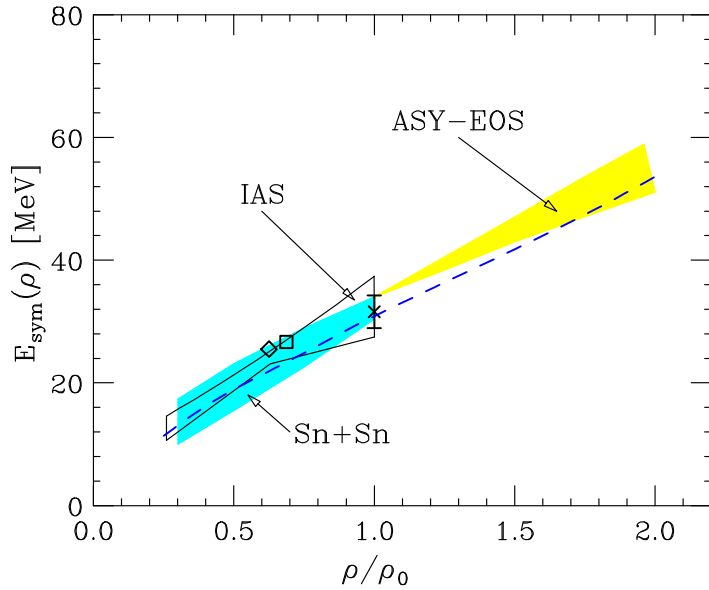


Figure 4. Density dependence of the symmetry energy of nuclear matter. The regions labelled ASY-EOS, Sn+Sn and IAS represent the results reported in Refs.[39], [40], and [41], respectively, while the symbols correspond to the analyses of Refs. [38] (cross with error bar), [42] (diamond), and [43] (square). The results of the CBF effective interaction approach are displayed by the dashed line.

context it has to be kept in mind that, being based on a non relativistic formalism, the CBF effective interaction approach is bound to predict a violation of causality—signaled by a value of the speed of sound in matter exceeding the speed of light—in the high-density limit.

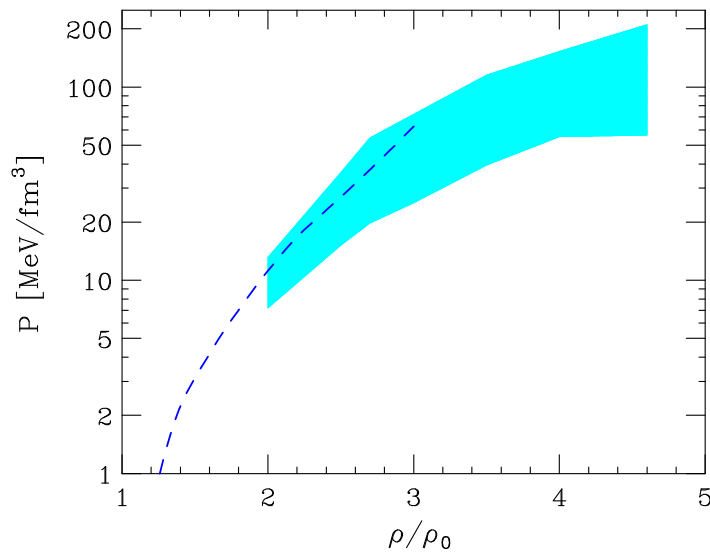


Figure 5. The dashed line illustrates the density dependence of the pressure of SNM obtained from the CBF effective interaction approach. The shaded area corresponds to the region consistent with the experimental flow data reported in Ref. [44].

3.4. Single particle spectrum and chemical potentials

At first order in the effective interaction, corresponding to the Hartree-Fock approximation, the energy spectrum of nucleons of type λ can be obtained from

$$e_{\lambda}(k) = \frac{k^2}{2m} + \rho \sum_{\mu} x_{\mu} \int d^3r \left[v_{\lambda\mu}^{\text{eff,d}}(\mathbf{r}) - j_0(kr) \ell(k_{F,\mu} r) v_{\lambda\mu}^{\text{eff,e}}(\mathbf{r}) \right], \quad (20)$$

with $j_0(x) = \sin x/x$. The above expression is often parametrized in terms of the effective mass m^* , defined as

$$\frac{1}{m^*} = \frac{1}{k} \left(\frac{de_\lambda}{dk} \right) \quad (21)$$

For vanishing temperature, equation (20) also gives the chemical potentials, which are simply related to the energy spectrum through $\mu_\lambda = e_\lambda(k_{F,\lambda})$.

Figures 6 and 7 show the density dependence of the ratios $m^*(k_F)/m$ and of the nucleon chemical potential in SNM (solid lines) and PNM (dashed lines).

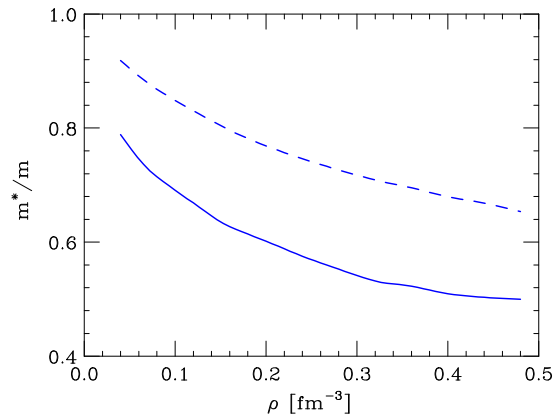


Figure 6. Density dependence of the ratio between the nucleon effective mass at $k = k_F$ and the bare nucleon mass. The solid and dashed lines correspond to SNM and PNM, respectively.

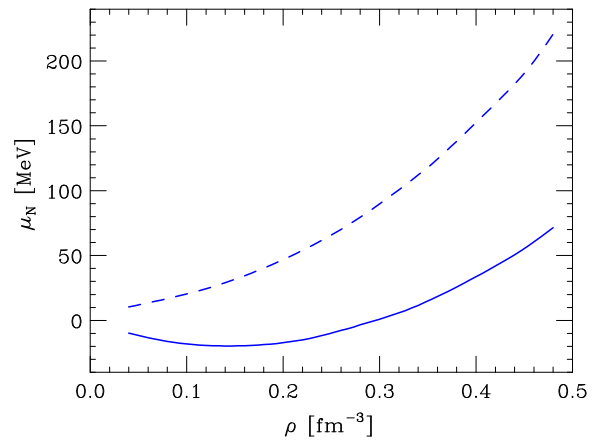


Figure 7. Density dependence of the nucleon chemical potential. The solid and dashed lines correspond to SNM and PNM, respectively.

3.5. Extension to nonzero temperature

To the extent to which thermal effects do not lead to modifications of the underlying nuclear dynamics, the approach described in this paper can be readily generalized to treat nuclear matter at nonzero temperature, by replacing the $T = 0$ Fermi distribution appearing in Eq. (15) with the corresponding distribution at temperature $T > 0$

$$n_\lambda(k, T) = \{1 + e^{\beta[e_\lambda(k) - \mu_\lambda]}\}^{-1}, \quad (22)$$

where $\beta = 1/T$, $e_\lambda(k)$ is the energy of a nucleon of type λ carrying momentum k , and the chemical potential μ_λ is determined by the constraint

$$\frac{1}{V} \sum_{\mathbf{k}\lambda} n_\lambda(k, T) = \rho_\lambda. \quad (23)$$

As an example, Figs. 8 and 9 show the temperature- and density-dependence of the Gibbs free energy per baryon of PNM and SNM, respectively, defined as

$$\frac{F}{A} = \frac{E_0 - TS}{A}, \quad (24)$$

where S denotes the entropy.

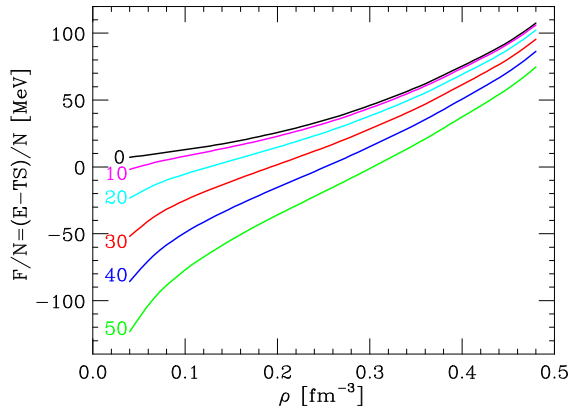


Figure 8. Density dependence of the Gibbs free energy per nucleon of PNM. The lines are labelled according to the temperature, T , expressed in units of MeV.

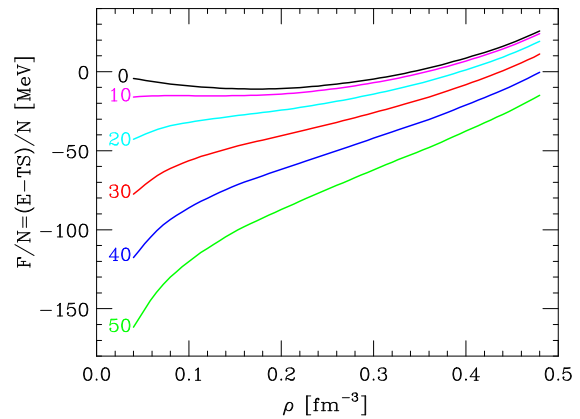


Figure 9. Same as in Fig. 8, but for SNM.

4. Summary and outlook

The results discussed in this paper provide convincing evidence that the effective interaction obtained from a realistic nuclear Hamiltonian using the CBF formalism and the cluster expansion technique is a powerful tool to carry out perturbative calculations of a variety of nuclear matter properties, ranging from the ground-state energy to the quasiparticle spectrum, the in-medium collision probability and the transport coefficients.

Unlike other advanced many-body approaches based on realistic models of nuclear dynamics at microscopic level—the applications of which are largely limited to calculations of the equation of state of SNM and PNM—the CBF effective interaction approach allows to study the properties of nuclear matter at large neutron excess, which are known to play a critical role in many astrophysical processes. In addition, under the assumption that thermal effects do not significantly affect strong interaction dynamics—which may be expected to be applicable at temperatures $T \ll m_\pi$, $m_\pi \sim 140$ MeV being the pion mass—it can be readily generalized to treat nuclear matter at nonzero temperature.

Ongoing and future applications to neutron star matter include the calculations of the shear and bulk viscosity coefficients, the superfluid gaps and the neutrino emission and absorption rates.

Acknowledgments

OB wishes to express his deepest gratitude to the organizers of “Compact Stars in the QCD phase diagram V”, as well as to the Gran Sasso Scientific Institute (GSSI). The work of AL is supported by the U.S. Department of Energy, Office of Science, Office of Nuclear Physics, under contracts DE-AC02-06CH11357.

References

- [1] Rikovska Stone J, Miller J C, Konciewicz R, Stevenson P D and Strayer M R 2003 *Phys. Rev. C* **68** 034324
- [2] Chabanat E, Bonche P, Haensel P, Meyer J and Schaeffer R 1997 *Nucl. Phys. A* **627** 710
- [3] Benhar O, Polls A, Valli M and Vidaña I 2010 *Phys. Rev. C* **81** 024305
- [4] Zhang H F, Lombardo U and Zuo W 2010 *Phys. Rev. C* **82** 015805
- [5] L Amundsen and E Østgaard 1985 *Nucl. Phys. A* **437** 487
- [6] J Wambach, TL Aisworth and D Pines 1993 *Nucl. Phys. A* **555** 128
- [7] Cowell S and Pandharipande V 2006 *Phys. Rev. C* **73** 025801
- [8] Benhar O and Valli M 2007 *Phys. Rev. Lett.* **99** 232501

- [9] Mecca A, Lovato A, Benhar O and Polls A 2015 *Phys. Rev. C* **91** 034325
- [10] Mecca A, Lovato A, Benhar O and Polls A 2016 *Phys. Rev. C* **93** 035802
- [11] Wiringa R B, Stoks V G J and Schiavilla R 1995 *Phys. Rev. C* **51** 38–51
- [12] Wiringa R B and Pieper S C 2002 *Phys. Rev. Lett.* **89** 182501
- [13] Fujita J and Miyazawa H 1957 *Prog. Theor. Phys.* **17** 360–365
- [14] Pudliner B S, Pandharipande V R, Carlson J and Wiringa R B 1995 *Phys. Rev. Lett.* **74** 4396–4399
- [15] A Gezerlis *et al* 2013 *Phys. Rev. Lett.* **111** 032501
- [16] M Piarulli *et al* 2015 *Phys. Rev.* **C91** 024003
- [17] J E Lynn *et al* 2016 *Phys. Rev. Lett.* **116** 062501
- [18] Jastrow R 1955 *Phys. Rev.* **98**(5) 1479–1484 URL <http://link.aps.org/doi/10.1103/PhysRev.98.1479>
- [19] Clark J W 1979 *Prog. Part. Nucl. Phys.* **2** 89 – 199
- [20] Fantoni S and Rosati S 1974 *Nuovo Cim.* **A20** 179–193
- [21] Pandharipande V R and Wiringa R B 1979 *Rev. Mod. Phys.* **51** 821–859
- [22] Fantoni S, Friman B L and Pandharipande V R 1982 *Nucl. Phys. A* **399** 51
- [23] Fantoni S and Pandharipande V R 1987 *Nucl. Phys. A* **473** 234
- [24] Fabrocini A and Fantoni S 1989 *Nucl. Phys. A* **503** 375
- [25] Benhar O, Fabrocini A and Fantoni S 1989 *Nucl. Phys. A* **505** 267
- [26] Benhar O, Fabrocini A and Fantoni S 1992 *Nucl. Phys. A* **550** 201
- [27] Fantoni S and Pandharipande V R 1988 *Phys. Rev. C* **37** 1697
- [28] Lagaris I and Pandharipande V R 1981 *Nucl. Phys. A* **359** 349
- [29] Lovato A, Losa C and Benhar O 2013 *Nucl. Phys.* **A901** 22–50
- [30] Lovato A, Benhar O, Gandolfi S and Losa C 2014 *Phys. Rev.* **C89** 025804
- [31] A Lovato, C Losa, and O Benhar 2013 *Nucl. Phys. A* **901** 22
- [32] A Lovato, O Benhar, S Gandolfi and C Losa 2002 *Phys. Rev. C* **89** 182501
- [33] RB Wiringa and SC Pieper 2014 *Phys. Rev. Lett.* **89** 025804
- [34] BS Pudliner, VR Pandharipande, J Carlson and RB Wiringa 1995 *Phys. Rev. Lett.* **74** 4396
- [35] Clark J W 1979 *Prog. Part. Nucl. Phys.* **2** 89
- [36] KE Schmidt and S Fantoni 1999 *Phys. Lett. B* **446** 99
- [37] M Baldo and F Burgio 216 *Prog. Part. Nucl. Phys.* **91** 203
- [38] B-A Li and X Han 2013 *Phys. Lett. B* **727** 276
- [39] P Russotto *et al* 2016 *Phys. Rev. C* **94** 034608
- [40] M B Tsang *et al* 2009 *Phys. Rev. Lett.* **102** 122701
- [41] P Danielewicz and J Lee 2002 *Nucl. Phys. A* **298** 1592
- [42] Brown B A 2014 *Phys. Rev. Lett.* **922** 1
- [43] Zhang Z and Chen L W 2013 *Phys. Lett. B* **726** 234 – 238
- [44] P Danielewicz, R Lacey, and W G Lynch 2002 *Science* **298** 1592